13 Magnetic Materials and Devices

Many of the world's bits are stored by orienting magnetic spins. The evolution of these magnetic storage devices is a good lesson in mature technology. For many years, confident and sensible predictions have shown why alternatives, such as optical and semiconductor storage, will soon replace magnetic media, but each year evolutionary innovations bring magnetic storage ever closer to fundamental physical limits and lead to revolutionary new applications. In the densest disks the bit spacing is on the order of 1 μm, reaching the diffraction limit for optical storage. This requires flying the recording head that close to the platter, which is comparable to the mean free path of an air molecule and hence in a regime where the air must be described by the discrete particles of kinetic theory rather than the continuum partial differential equations of hydrodynamics. Terabytes fit in drives that are just a few inches big, with costs that have dropped from thousands to hundreds of dollars [Grochowski *et al*., 1993]. These improvements are the result of a combination of accumulated experience with this system, sophisticated study of the underlying mechanisms, and some luck in how nature responds to such aggressive scaling [Mallinson, 1996]. Surely a time will come when we will stop using spinning platters of what is essentially rust for information storage, but that time has receded much further than was once thought.

Magnetism is a surprisingly complex and still incompletely understood subject. This chapter therefore starts with a review of the basic phenomenology of magnetic materials, and an introduction to the mechanisms that cause it. These are then applied to explain magnetic storage, and device applications of magnetic materials.

13.1 MAGNETISM

In Chapter 6 we saw that the energy density in a field is

$$U \equiv \frac{1}{2}(\vec{E} \cdot \vec{D} + \vec{B} \cdot \vec{H}) \quad \left(\frac{\mathrm{J}}{\mathrm{m}^3}\right) \quad , \tag{13.1}$$

and that in a magnetic material

$$\vec{B} = \mu\vec{H} = \mu_0\mu_r\vec{H} = \mu_0(1 + \chi_m)\vec{H} = \mu_0(\vec{H} + \vec{M}) \quad , \tag{13.2}$$

where $\vec{B}$ is the magnetic flux density, $\vec{H}$ is the magnetic field strength, and $\vec{M}$ is the magnetization. The magnetization is equal to the magnetic moment $\vec{m}$ of the material

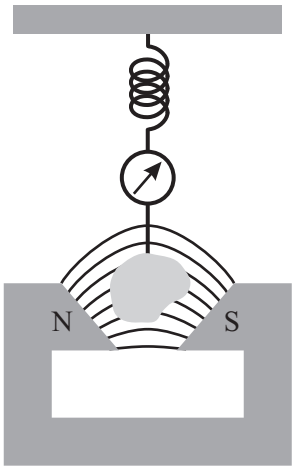

Figure 13.1. Measurement of permeability by an inhomogeneous field.

per volume:

$$\vec{M} = \frac{\vec{m}}{V} \quad . \tag{13.3}$$

Unlike most engineering practice, in the study of magnetic media CGS units are most commonly used because the magnitudes of the quantities are more appropriate. MKS (SI) magnetic fields are measured in amps per meter; the conversion to the CGS (EM) unit, the *oersted*, is

$$H: \ 1 \ \frac{\mathrm{A}}{\mathrm{m}} = \frac{4\pi}{10^3} \ \mathrm{Oe} \quad . \tag{13.4}$$

The SI flux density is measured in tesla; the conversion to *gauss* is

$$B: \ 1 \ \mathrm{T} = 10^4 \ \mathrm{G} \quad . \tag{13.5}$$

Now consider what happens if a material is brought into a magnetic field that has a gradient in the z direction. This might be created by a magnet with tapered pole pieces, shown in Figure 13.1. If the material has a volume V, assumed to be small compared to the length scale of the gradient, then the change in energy after it is brought into the field is equal to the field energy stored in the material minus the energy that was there beforehand:

$$\begin{aligned} \Delta E &= \frac{1}{2}\int_{\text{material}} \vec{B}\cdot\vec{H}\, dV - \frac{1}{2}\int_{\text{no material}} \vec{B}\cdot\vec{H}\, dV \\ &= \frac{1}{2}V\mu_0\mu_{\mathrm{r}}H^2 - \frac{1}{2}V\mu_0 H^2 \\ &= \frac{1}{2}V\mu_0(\mu_{\mathrm{r}} - 1)H^2 \\ &= \frac{1}{2}V\mu_0\chi_{\mathrm{m}}H^2 \quad . \end{aligned} \tag{13.6}$$

There will be a force on the material, measured by the scale in Figure 13.1, that is equal

to the gradient of this energy

$$F = -\frac{d\Delta E}{dz}$$
$$= -V\mu_0\chi_m H\frac{dH}{dz} \quad . \tag{13.7}$$

The force will be proportional to the magnetic susceptibility χ_m, which is equal to the relative permeability μ_r minus 1. This technique, proposed by Faraday, provides a simple way to measure the permeability of a material. It leads to the following unexpected experimental result: some materials (*diamagnetic*, *superconducting*) move up the gradient towards the weaker field, and some (*paramagnetic*, *ferromagnetic*, *ferrimagnetic*) move down it towards the stronger field. Diamagnetic materials have a small negative susceptibility ($\mu_r = 0.99996$ for Au), paramagnetic materials have a small positive susceptibility ($\mu_r = 1.00002$ for Al), and ferromagnetic and ferrimagnetic materials have a huge positive susceptibility ($\mu_r \sim 10^4$ for steel). In a superconductor, the *Meissner effect* requires that there be no flux lines in the material. This implies that $\vec{B} = 0$ and so

$$\vec{H} = -\vec{M} \Rightarrow \chi_m = \frac{M}{H} = -1 \quad . \tag{13.8}$$

This susceptibility is many orders of magnitude larger than that for a normal diamagnetic material; this strong repulsion can be used for magnetic levitation of bearings and vehicles [Nakashima, 1998].

Why do materials have such different opinions about how to behave in a magnetic field? We now turn to the microscopic origin of magnetic phenomena. Ferromagnetism is the most important mechanism for magnetic storage, but it will be instructive to relate all of them.

13.1.1 Diamagnetism

Lenz's Law states that a time-varying magnetic field induces a current in a loop that acts to oppose the field; diamagnetism comes from this effect operating on the electrons in an atom. Although this is a quantum system, a simple model due to Langevin is in good quantitative agreement with experimental measurements. Viewed semiclassically, the magnetic moment of an electron orbiting a nucleus is

$$m = I\,A = \frac{qv}{2\pi r}\,\pi r^2 = \frac{qvr}{2} \quad . \tag{13.9}$$

A time-varying field threading this loop gives rise to an induced potential around the loop

$$\mathcal{V} = -\frac{d\Phi}{dt} = -\frac{d(BA)}{dt} = -\mu_0\frac{d(HA)}{dt} \quad , \tag{13.10}$$

taking the magnetic field direction to be normal to the loop. This accelerates the electron by

$$a = \frac{dv}{dt} = \frac{F}{m_e} = \frac{q\mathcal{V}}{2\pi r m_e} = -\mu_0\frac{qr}{2m_e}\frac{dH}{dt} \quad . \tag{13.11}$$

Integrating both sides as the field is ramped up from 0 to H in a time T gives the total

change in velocity

$$\int_0^T \frac{dv}{dt}\,dt = \int_0^T -\mu_0 \frac{qr}{2m_e}\frac{dH}{dt}\,dt$$
$$\Delta v = -\mu_0 \frac{qrH}{2m_e} \quad , \tag{13.12}$$

which in turn gives the change in the moment

$$\Delta m = \frac{q\Delta v r}{2} = -\mu_0 \frac{q^2 r^2 H}{4m_e} \quad . \tag{13.13}$$

The magnetization caused by this induced moment is

$$M = \frac{m}{V} = -\mu_0 \frac{q^2 Z r^2 H}{4m_e V} \quad , \tag{13.14}$$

where V is the volume of the atom, and the factor of Z has been added to account for multiple electrons in the atom. The susceptibility is then

$$\chi_m = \frac{M}{H} = -\mu_0 \frac{q^2 Z r^2}{4m_e V} \quad . \tag{13.15}$$

Even though this estimate has ignored both thermodynamics and quantum mechanics, it gives numbers that are in line with observed values for diamagnetic materials (Problem 13.1), and shows why diamagnetism is not strongly temperature dependent.

13.1.2 Paramagnetism

The effective current loop used in the preceeding calculation is not fixed in space; under an applied field it can change its orientation as well as speed up or slow down. For the simplest quantum mechanical case of non-interacting spin-1/2 magnetic moments, this corresponds to flipping between states parallel and antiparallel to the field (Chapter 16). If the magnetic moment is m, the energy of the two states is $\pm mB$. If the density of these moments is n, then the magnetization is found from the expected value of the spin orientation

$$\begin{aligned} M &= nm\langle s \rangle \\ &= nm\frac{\sum_{s=-1,1} s e^{-E_s/kT}}{\sum_{s=-1,1} e^{-E_s/kT}} \\ &= nm\frac{e^{mB/kT} - e^{-mB/kT}}{e^{mB/kT} + e^{-mB/kT}} \quad . \end{aligned} \tag{13.16}$$

mB is usually much smaller than kT, so the exponentials can be expanded as $1 \pm mB/kT$, giving

$$\begin{aligned} M &= \frac{nm^2 B}{kT} \\ &= \frac{nm^2 \mu_0 H}{kT} \end{aligned} \tag{13.17}$$

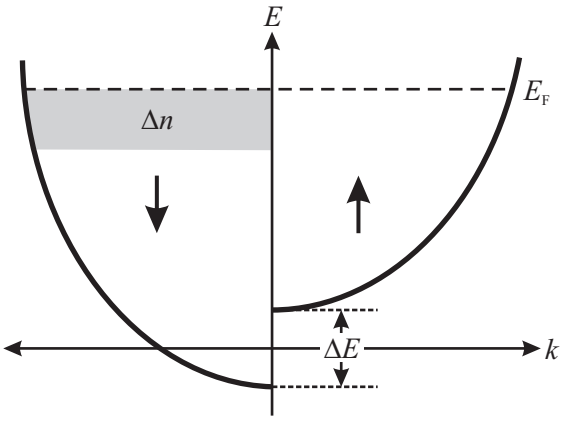

Figure 13.2. Spin band splitting in a field.

or

$$\begin{aligned}\chi_m &= \frac{M}{H} \\ &= \frac{nm^2\mu_0}{kT} \\ &\equiv \frac{C}{T} \quad .\end{aligned} \tag{13.18}$$

This is *Curie's Law* and the constant C is (can you guess?) the *Curie constant*.

Curie's Law might be expected to apply to the conduction electrons in a metal, which have a spin magnetic moment of

$$\mu_B = \frac{e\hbar}{2m_e} = 9.274\times10^{-24}\ \frac{\mathrm{J}}{\mathrm{T}} \quad , \tag{13.19}$$

but the susceptibility of most metals is found to be relatively independent of temperature rather than inversely proportional to it. Pauli solved this mystery by pointing out that the derivation of Curie's Law used a canonical partition function, which is appropriate only in the high-temperature limit. Otherwise, the Fermi–Dirac distribution must be used.

The band diagrams in Chapter 11 were drawn as a function of momentum, with each momentum state containing a spin-down and a spin-up state. Figure 13.2 replots a band diagram with all the spin-down states on the left and the spin-up states on the right; each spin state is now associated with $+k$ and $-k$ momentum states. An applied field will split the spin energies. Because the Fermi energies must remain equal, some electron spins flip (assuming that there are available states for them to go into). The number of electrons transferred is approximately equal to the energy split times the density of states at the Fermi energy $n(E_F)$. The two populations will equalize when half the difference is transferred, but there are two momentum states for each spin state:

$$\Delta n = \Delta E\ n(E_F) = B\mu_B n(E_F) \quad . \tag{13.20}$$

The magnetization is the induced moment per volume

$$M = \frac{m}{V} = \mu_B\ \Delta n = \mu_B^2 B n(E_F) \quad , \tag{13.21}$$

therefore the susceptibility is

$$\chi_{\mathrm{m}} = \frac{M}{H} = \mu_0 \mu_{\mathrm{B}}^2 n(E_{\mathrm{F}}) \quad . \tag{13.22}$$

This is the spin paramagnetism of a metal. It is positive, roughly temperature-independent, and it will vanish if the density of states vanishes at the Fermi energy because the valence band is full. A paramagnetic material still has the diamagnetic magnetization from the electron orbits, but if the paramagnetic magnetization is large enough it will dominate. This is one example of how materials can be paramagnetic (partially-filled conduction band), diamagnetic (filled valence band), or have little susceptibility (diamagnetism cancels paramagnetism).

Other than obeying Fermi–Dirac statistics, Pauli paramagnetism assumes that the spins are independent. One sign of the failure of this approximation is that in many materials Curie's Law is empirically found to need an offset

$$\chi_{\mathrm{m}} = \frac{C}{T - T_{\mathrm{C}}} \quad . \tag{13.23}$$

This is the *Curie–Weiss* Law. T_{C} is the *Curie temperature*, and can be quite large: 1043 K in iron, for example. If it is defined in terms of the Curie constant as $T_{\mathrm{C}} = \lambda C$, the susceptibility can be rewritten as

$$\begin{aligned} \chi_{\mathrm{m}} &= \frac{M}{H} \\ &= \frac{C}{T - \lambda C} \\ HC &= MT - M\lambda C \\ \frac{C}{T} &= \frac{M}{H + \lambda M} \quad . \end{aligned} \tag{13.24}$$

This recovers the original form of Curie's Law, if we assume that the spins see a local field λM added to the applied field H. The offset λM is called the *molecular field*, and to understand it we must understand the origin of ferromagnetism and its relatives.

13.1.3 Ferro-, antiferro-, and ferri-magnetism

Diamagnetism and paramagnetism can arise from a range of mechanisms, all relatively weak. Ferromagnetic materials behave very differently in an applied field: the response is large and *hysteretic*. This dependence of the present state of the sample on its past history provides the memory mechanism needed for magnetic storage. The magnetization of a ferromagnet could be measured by the apparatus in Figure 13.1, or its modern cousin the *Vibrating Sample Magnetometer* (*VSM*) that vibrates the sample in a fixed applied field and listens in nearby pickup coils to the signal due to the moving magnetization. If the induced magnetization is plotted as a function of the applied field, the result will look something like Figure 13.3. It is still true by definition that $B = \mu_0(H + M)$, but now the simple ratio $\mu = B/H$ must be replaced with the *differential permeability* $\mu = dB/dH$.

As the applied field is ramped up, the magnetization grows until it reaches a saturation value M_{S} that is independent of the field. When the field is brought back to zero a *remnant*

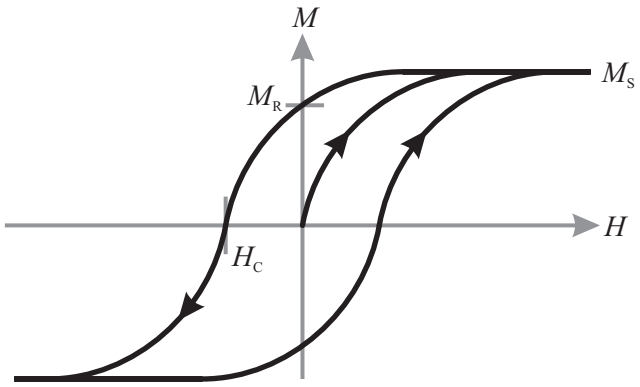

Figure 13.3. A hysteresis loop.

magnetization M_R remains, and if the field is further decreased to the *coercivity* $-H_C$ the remnant magnetization will be removed. This is called a *hysteresis loop*; it can also be plotted as B vs H.

Such persistent magnetic ordering cannot be explained by magnetic forces, which are typically much smaller than kT. They can actually be ignored; to understand this we must turn to the much larger electrostatic interactions (Problem 13.2), and quantum mechanics. Let's start with the simplest possible model for a solid, two nuclei and two electrons. Although this is really just a hydrogen molecule, it's enough to introduce the origin of ferromagnetism.

Call the nuclei a and b, and the electrons 1 and 2. If we isolate one of the atoms, say electron 1 around nucleus a, and assume that the nucleus is so massive that it doesn't move, the Hamiltonian is just

$$\mathcal{H}_a = \frac{p_1^2}{2m} - \frac{e^2}{r_{1a}} \quad , \tag{13.25}$$

where r_{1a} is the distance between electron 1 and nucleus a. Let $\varphi_a(\vec{x}_1)$ be the lowest-energy eigenfunction of this Hamiltonian.

Now bring the atoms closer together. The single-electron eigenfunctions will no longer be eigenfunctions of the joint Hamiltonian, but we can use them as a basis to build those up. These joint wave functions $\psi(1,2)$ must satisfy two essential constraints. Because quantum particles are *indistinguishable*, expectation values must not change if the particles are interchanged, so

$$|\psi(1,2)|^2 = |\psi(2,1)|^2 \quad . \tag{13.26}$$

And because electrons are fermions, the wave function must be antisymmetric, changing sign if the electrons are swapped

$$\psi(1,2) = -\psi(2,1) \quad . \tag{13.27}$$

ψ must describe both the spin and spatial degrees of freedom of the electrons. Chapter 16 will work out the form of the spin states for two electrons; these will be either symmetric or antisymmetric under particle interchange. This means that the corresponding spatial wave functions must be either antisymmetric or symmetric, to preserve the overall

antisymmetry. We can construct such states from our single-electron eigenfunctions by combining them as

$$\psi(\vec{x}_1, \vec{x}_2) = \varphi_a(\vec{x}_1)\varphi_b(\vec{x}_2) \pm \varphi_a(\vec{x}_2)\varphi_b(\vec{x}_1) \quad . \tag{13.28}$$

The plus sign goes with the antisymmetric spin state, and the minus sign with the symmetric spin state. These will no longer be eigenfunctions of the joint Hamiltonian, but will be a good approximation as the atoms begin to come together, and will be part of a complete basis set to expand an arbitrary solution.

The Hamiltonian for the joint system becomes

$$\mathcal{H} = \underbrace{\frac{p_1^2}{2m} + \frac{p_2^2}{2m} - \frac{e^2}{r_{1a}} - \frac{e^2}{r_{2b}}}_{\mathcal{H}_0} + \underbrace{\frac{e^2}{r_{ab}} + \frac{e^2}{r_{12}} - \frac{e^2}{r_{1b}} - \frac{e^2}{r_{2a}}}_{\mathcal{H}_{\text{int}}} \quad . \tag{13.29}$$

$\mathcal{H}_0$ is the sum of the Hamiltonians for the individual atoms, having the single-electron eigenstates, and $\mathcal{H}_{\text{int}}$ is the interaction Hamiltonian that arises from bringing the atoms together. The energy associated with the interaction is $E_{\text{int}} = \langle\psi|\mathcal{H}_{\text{int}}|\psi\rangle$. If we evaluate this for our basis wave function,

$$\begin{aligned} E_{\text{int}} &= \langle\psi|\mathcal{H}_{\text{int}}|\psi\rangle \\ &= \int\int \psi^* \left(\frac{e^2}{r_{ab}} + \frac{e^2}{r_{12}} - \frac{e^2}{r_{1b}} - \frac{e^2}{r_{2a}}\right) \psi \; d\vec{x}_1 d\vec{x}_2 \\ &= 2\int\int |\varphi_a(\vec{x}_1)|^2 |\varphi_b(\vec{x}_2)|^2 \left(\frac{e^2}{r_{ab}} + \frac{e^2}{r_{12}} - \frac{e^2}{r_{1b}} - \frac{e^2}{r_{2a}}\right) d\vec{x}_1 d\vec{x}_2 \\ &\pm 2\int\int \varphi_a^*(\vec{x}_1)\varphi_b^*(\vec{x}_2)\varphi_a(\vec{x}_2)\varphi_b(\vec{x}_1) \left(\frac{e^2}{r_{ab}} + \frac{e^2}{r_{12}} - \frac{e^2}{r_{1b}} - \frac{e^2}{r_{2a}}\right) d\vec{x}_1 d\vec{x}_2 \\ &= E_{\text{overlap}} \pm E_{\text{exchange}} \quad . \end{aligned} \tag{13.30}$$

The first term is the *overlap* integral, and the second is the *exchange* integral. Here is the essential point: the preferred spin orientation will be the one that minimizes the contribution from the exchange integral. The relative orientation of the electron spins determines the symmetry of the spin wave function. It in turn constrains the spatial wave function to be either symmetric or antisymmetric, determining the sign of the exchange integral. This integral is a function of electrostatic forces, setting an energy scale much larger than the magnetic forces associated with the spin ordering. This is how electrostatic interactions lead to stable magnetic ordering.

The overlap integral is really a manifestation of the Pauli exclusion principle. The electrons can't be in the same state, leading to an effective force between them. Although its origin lies in the foundations of symmetry in quantum mechanics, its consequence is a very real interaction. For spin 1/2, in Chapter 16 we will see that the dot product $\vec{S}_1 \cdot \vec{S}_2$ of two spins $\vec{S}_1$ and $\vec{S}_2$ can have eigenvalues of $-3/4$ for the antisymmetric spin state or $+1/4$ for the symmetric state. Through the exchange integral, these spin states are associated with overall energies $E_{\text{antisymmetric}}$ and $E_{\text{symmetric}}$. This relationship can be described by an effective spin Hamiltonian

$$\mathcal{H}_{\text{spin}} = \frac{1}{4}(E_{\text{antisymmetric}} + 3E_{\text{symmetric}}) - (E_{\text{antisymmetric}} - E_{\text{symmetric}})\vec{S}_1 \cdot \vec{S}_2 \quad , \tag{13.31}$$

verified by plugging in $\vec{S}_1 \cdot \vec{S}_2 = -3/4, +1/4$. Dropping the constant that does not depend on the spins, calling the prefactor J, and generalizing to more than two spins gives the *Heisenberg Hamiltonian*

$$\mathcal{H}_{\text{spin}} = -\sum_{i,j} J_{ij} \vec{S}_i \cdot \vec{S}_j \quad . \tag{13.32}$$

This interaction is called *$\mathcal{J}$ coupling*. If J is positive, as it is for the metals Fe, Co, and Ni, then the spins will want to point in the same direction, giving *ferromagnetic* ordering.

In an *antiferromagnet* such as Mn or Cr the exchange energy is negative, therefore neighboring spins alternate orientation and there is no net moment even though there is long-range magnetic order. A *ferrimagnet* is a ceramic oxide that has a spontaneous moment but is a good insulator. The moment arises because it has an antiferromagnetic coupling, but there are interpenetrating spin-up and spin-down lattices that have different moments that do not cancel. Most common ferrimagnets are made from materials containing iron oxides, called *ferrites*. Because they do not conduct, they do not screen electric fields or have eddy current heating, and so they are useful for a range of microwave applications as well as guiding flux in coils. One example is the microwave equivalent of optical Faraday rotation, which is used in a "magic T" to steer microwave signals in different directions depending on whether they arrive at the input or the output port. This apparent violation of reversibility is possible because magnetic interactions break time reversal invariance, since the sign of time appears in the velocity in the basic $\vec{v} \times \vec{B}$ law. Cables are often wrapped around ferrites, such as the beads on computer monitor cables, to add inductance to filter out unwanted high-frequency components.

Equation (13.32) can include terms coupling non-adjacent spins. The exchange interaction between overlapping wave functions in equation (13.30) is called *direct exchange*; it's also possible for an exchange interaction to pass through many intervening particles. This is called *indirect exchange*. An important example occurs in NMR, where bonding electrons mediate an exchange interaction between atomic nuclei [Ernst *et al*., 1994], and indirect exchange is the origin of the strength of rare-earth magnets [Buschow, 1991]. Although a great deal is known about the behavior of the Heisenberg Hamiltonian, quantitatively calculating the J_{ij}'s and its solution from first principles remain dauntingly open problems because of the challenge of handling these many-body effects beyond the independent electron approximation [Mattis, 1988].

At high temperatures, ferromagnets become paramagnets when thermal excitations become more significant than the exchange energy. This is observed to be a sharp transition, with the saturation magnetization vanishing at the Curie temperature T_C (Figure 13.4). Likewise, antiferromagnets become paramagnets above the *Néel temperature*. As a ferromagnet is lowered below its Curie temperature, the saturation magnetization reaches a limiting value when all of the spins in the material are aligned.

The remnant magnetization is what's left of the saturation magnetization after the applied field is taken away. If it is large, the material is said to be *hard* and is useful as a permanent magnet. If it is small, the material is said to be *soft*. Microscopically, these materials differ in their local anisotropy. Because the energy stored in a magnetic field is

$$E = \frac{1}{2\mu} \int B^2 \, dV \quad , \tag{13.33}$$

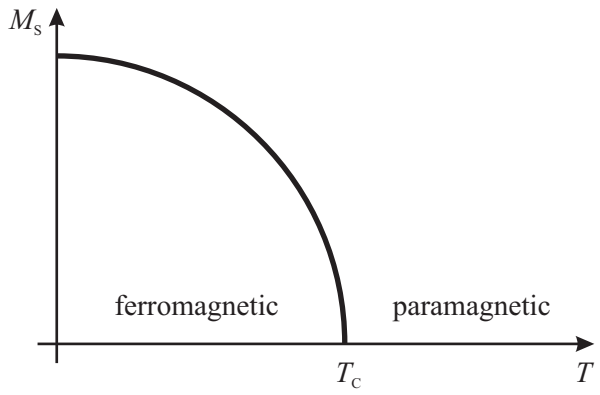

Figure 13.4. The temperature dependence of the saturation magnetization.

the energy will be minimized if the magnetic flux density is greatest in regions of high permeability. Therefore, materials with high permeability "pull in" the field from around them; that is why this property is called permeability. It can be used to guide the field in a recording head or transformer core. Since there is dissipation associated with a hysteresis loop (Problem 13.5), these applications use a soft magnetic material with a narrow hysteresis loop. This is particularly true of *metallic glasses* that are formed by rapidly quenching metallic alloys to prevent the growth of crystalline ordering. Transformer core materials are also often laminated from thin sheets; this reduces eddy current heating if the laminations are perdendicular to the direction electrons are accelerated by the field.

Because of the exchange energy, in a ferromagnet the atomic spins are locally aligned forming *domains*. However, the domain size is usually much smaller than the sample size because of competing factors such as thermal fluctuations which can reorient domains, and because of the energy stored in the fields produced by the domains. To see the latter effect, consider what happens to a sample that is initially homogeneously magnetized (Figure 13.5). There is a large energy that is stored in the external return flux, which can be reduced by splitting the spins into two opposite domains so that the return flux does not have to travel as far. This can be further reduced by splitting into four domains, and so forth. The process does not continue indefinitely, because at the boundary between domains the spins require a few hundred lattice spacings to change direction in what is called a *Bloch wall*. Through the dot product, the exchange energy is proportional to the cosine of relative spin orientations θ. In the limit of a small misalignment this can be expanded as $1 - \theta^2$. Expanding the wall over multiple spins incurs a linear increase in energy from the number of spins, but saves a quadratic amount of energy by reducing the relative angles. This spreads the wall out, up to a size limited by favorable global spin alignment. The final domain size is a result of the tradeoff among all of these mechanisms; characteristic sizes are 1–100 μm. A *magnetic bubble* is a small domain that is just a single loop of a Bloch wall; magnetic bubbles were once of interest for non-volatile memories, but were limited by the speed at which they could be moved.

Each trip around a hysteresis loop starts with most of the spins pointing in the same direction; because of temperature some will point in other directions. As an external field is swept, domains with spins pointing in the opposite directions will be seeded and grow,

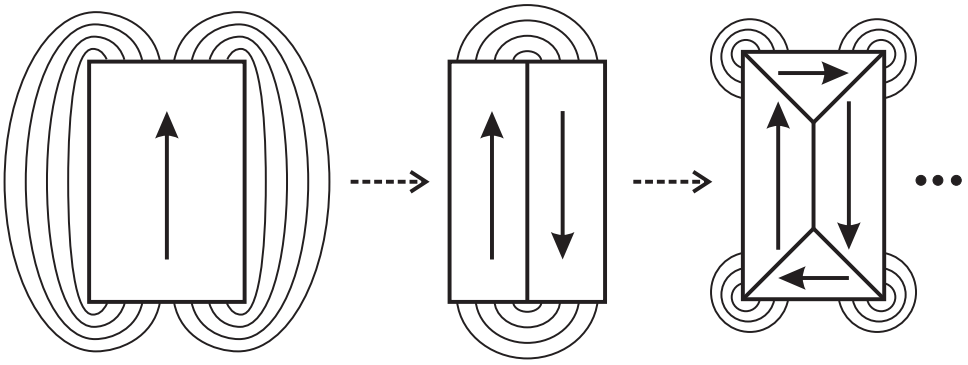

Figure 13.5. Magnetic domains reduce return flux energy.

eventually taking over the entire sample. This process takes time; moving the field quickly has little effect. Therefore the shape of a hysteresis loop will also depend on how fast the field is changed, reaching a limit in the case of slow field changes. If the field does not reach the saturation magnetization then some domains will be left with opposite spins. This is why slowly reducing an oscillating magnetic field will demagnetize a sample. If a hysteresis loop is examined in detail, the continuous curve is actually made of discrete steps called *Barkhausen steps*. These arise from discontinuous jumps in the size of the magnetic domains; within a single step the change in the magnetization is reversible.

13.2 MAGNETIC RECORDING

Magnetic recording started with Valdemar Poulsen crudely recording speech on a steel wire in 1898 by using a electromagnet hung from a trolley running along the wire. Since then the sophistication of the media and recording systems has progressed profoundly, but the basic principle is unchanged: write the message as magnetization in a suitable media, and then later detect that magnetization. Because thermal fluctuations can move domain walls, all magnetic media will eventually erase themselves if left at room temperature; like most digital media they are not suitable for very long-term archival storage unless there is regular error correction.

13.2.1 Magnetic Media

Most magnetic media consist of ferrite particles in a binder. To give the sharpest and most stable hysteresis curve, the particles are chosen to be just small enough ($\sim$1 μm) so that they cannot support a transverse domain wall. The oldest material used, and still one of the most common, is the phase γ-Fe_2O_3 (*gamma ferric oxide*). It has a coercivity of 300 Oe and a Curie temperature of 600 °C, although it undergoes a phase transition at 400 °C. *Chromium dioxide* (CrO_2) became popular for analog recording because of its higher coercivity of 450 Oe, but this comes at the price of a Curie temperature reduced to just 128 °C. One of the highest coercivities occurs in $BaFe_{12}O_{19}$ at $\sim$6000 Oe, making it useful for magnetic stripes on credit cards. This is actually too large to be useful for

recording; Co–Ti is added to reduce the coercivity down to ~1000 Oe. Other materials can be added to improve the mechanical properties of the medium, such as ceramic particles that help protect it from hard disk head crashes (discovered accidently from using ceramic materials to grind iron oxide powder in a ball mill).

Magnetic tape is made by dispersing the ferrite in a solvent and binder and spreading it on a substrate, typically a *polyester* such as *mylar*, that is ~1 mil thick (0.001 inch, 25.4 μm). A strong field is applied to orient the particles along the tape axis, the solvent is dried by heating, and then the tape is compressed and polished between rollers. Floppy disks are made in a similar manner except that the particles are randomly aligned, leading to a smaller remnant magnetization on the order of 1000 G instead of 1500 G. About 2000 square miles of recording media were coated in 1990.

The most sophisticated hard disks replace this process by the vacuum deposition of thin magnetic films such as CoCr or CoNi. A film of 500 Å can have a coercivity of 1000 Oe, and when deposited on a glass or diamond-turned Al substrate it can be flat and smooth enough to permit extremely close head–platter distances. Thin films also have the advantage of hysteresis curves that are almost rectangular, so that the transition between orientations is very sharp. Further improvements to the media are coming from lithographic patterning to eliminate the interaction energy between adjacent bits, and storing the bits with a vertical domain orientation to pack them together more closely [Bertram *et al*., 1998; Todorovic *et al*., 1999]. Such refinements have brought magnetic recording over a density of 100 Gbit/in^2, challenging the diffraction limit of optical storage.

13.2.2 Magnetic Recording

The most common recording head was an inductor wound around a loop of a magnetically soft permeable material such as *permalloy* ($Ni_{78}Fe_{22}$), which has a permeability over ~10^5. The large permeability guides the field to a gap that produces a fringing field that is used for reading and writing (Figure 13.6). In a *laminated head* sheets of permalloy approximately 1 mil thick are stacked and pressed; this helps confine the flux within the head because there is a cost for it to cross between laminations, and it reduces eddy current losses. The gap is polished and then filled with a spacer such as glass.

If an analog signal to be recorded was applied directly to the write head, the recording would be dreadful because of the hysteresis of the media. This can be cured by adding a high-frequency *bias* signal, typically in the range of 100–400 kHz and with an amplitude ~10 times that of the desired signal. The bias takes the media quickly around the hysteresis loop. With no write signal, this just swings between the saturation magnetizations. However, when the write signal is added, one side of the cycle is slightly less magnetized than the other, and it was experimentally discovered that this difference is surprisingly linear in the write signal as long as it is not too large. The high-frequency bias is removed when the recording is read because it is far out of the bandwidth of the read electronics.

Permalloy is a mechanically soft material and so permalloy heads suffer from wear and poor dimensional control. Much more durable heads, such as those needed for video recording, are made from a ferrite with a layer of SiO_2 grown at an interface to provide the gap. The most precise heads are made by thin film deposition on a substrate of a

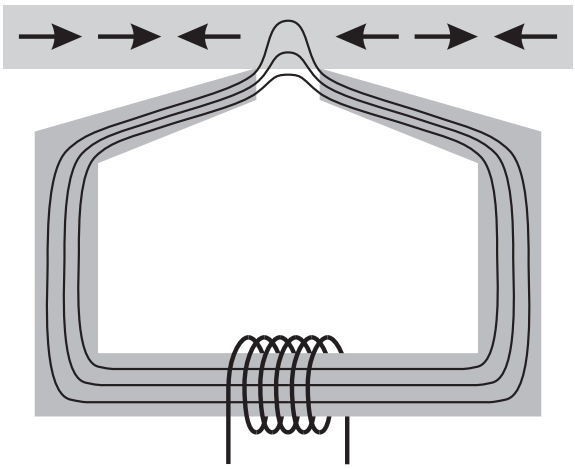

Figure 13.6. An inductive recording head.

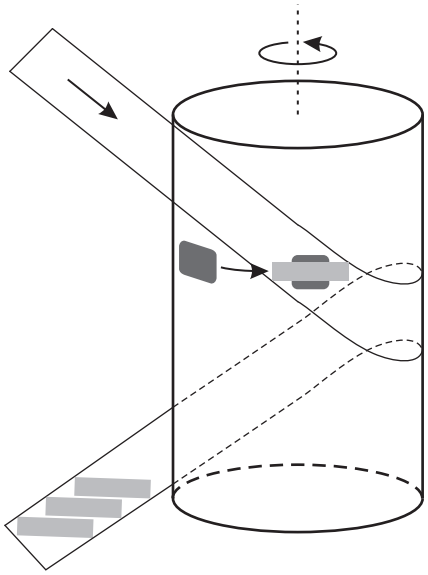

Figure 13.7. Tracks written by helical scan magnetic recording.

permalloy layer, a layer of copper coils, a top permalloy layer, and then a SiO_2 overlayer; these are used in very high density computer disks.

Videotape and digital audio tape systems require high frequencies, $\sim$10 MHz. Even if the read and write electronics could operate at these frequencies, the corresponding wavelength of the recording on the tape would be too short for the spins to follow. A solution to this problem, developed by the Ampex Corporation around 1956, is to move the head relative to the tape so that the relative speed between the head and the tape can be much higher. This can be done with *helical scanning*, shown in Figure 13.7.

The heads that have been discussed so far use inductive coils for picking up the signal. As the size of the area that is written decreases it becomes necessary to use more and

more turns in the coil to maintain an adequate signal strength, but this increases the inductance, slowing down the response of the head. Also, for a constant speed drive the signal strength will vary from the edge to the center of the platter because the relative velocity between the platter and the head changes. An alternative is *magnetoresistive* heads, which use a material that has a resistance that depends on an applied magnetic field. A common example is permalloy, which changes its resistance by a few percent in the fields used for recording. Aside from having no inductance, magnetoresistive heads have the great advantage that the response does not depend on the relative velocity of the head and the substrate, and so it is expected that they will become dominant for high-performance applications.

There has been a great deal of interest in *giant magnetoresistance* materials, such as multilayer or granular structures of NiFeCo/Cu, which can have magnetoresistances of tens of percent [Baibich *et al*., 1988]. These operate by using the field to modify spin-dependent electron transport properties [Parkin, 1994]. Even larger magnetoresistance is seen in materials related to $La_{0.7}Ca_{0.3}MnO_3$ [Ramirez *et al*., 1997]. This change can be 100% or more, and has come to be called *colossal magnetoresistance* (of course).

13.2.3 Recording Systems

Commercial magnetic storage systems have ranged from pocket cassette players up to petabyte servers; some sample parameters for examples across this history are listed below. As with all other aspects of magnetic storage, it is hard to beat mature solutions refined by big markets.

Audiotape (cassette)

- Frequency range: 20 Hz–20 kHz (CrO_2 tape)
- Bias frequency: 100 kHz
- SNR: 80 dB (Dolby S)
- Tape speed: 1-7/8 inches per second
- Shortest wavelength: 2 μm

Videotape (VHS-SP)

- Tape speed: 1-5/16 inches per second
- Tape width: 0.5 in
- Track pitch: 58 μm
- Track angle from horizontal: 6°
- Drum diameter: 2.45 in
- Drum rotation rate: 1800 revolutions per minute
- Luminance modulation: 3.4–4.4 MHz (FM)
- SNR: 42 dB
- Relative head speed: 220 inches per second
- Shortest wavelength: 1 μm

Magnetic Storage Tape (LTO-8)

- Capacity: 12 TB
- Length: 960 m

- Width: 12.65 mm
- Thickness: 5.6 um
- Media: BaFe
- Total tracks: 6656
- Max speed: 360 MB/s
- Linear Density: 20668 bits/mm

Floppy Disk (3.5 in HD)

- Formatted capacity: 1.44 MB
- Data transfer rate: 500 kbit/s
- Bit density: 17434 bits per inch
- Track density: 135 tracks per inch
- Rotation rate: 300 revolutions per minute

Hard Disk (Western Digital Ultrastar DC HC620)

- Disk size: 3.5 in
- Number of platters: 8
- Capacity: 14 TB
- Areal density: 1034 Gbit per square inch
- Rotation rate: 7200 revolutions per minute
- Sustained transfer rate: 267 MB/s
- Atmosphere: helium

13.3 HALL EFFECT

13.3.1 Classical

Hall effect

$$\vec{F} = q(\vec{E} + \vec{v}\times\vec{B}) \tag{13.34}$$

in equilibrium $\vec{F} = 0$

$$E_y = -v_x B_z \tag{13.35}$$

potential across width w

$$E_y = -\frac{V_H}{w} \tag{13.36}$$

equate

$$V_H = v_x B_z w \tag{13.37}$$

current through width w thickness t carrier density n charge e

$$I_x = ntwv_x e \tag{13.38}$$

$$V_H = \frac{I_x B_z}{nte} \tag{13.39}$$

Hall coefficient

$$\begin{aligned} R_H &= \frac{E_y}{j_x B_z} \\ &= -\frac{V_H}{w j_x B_z} \\ &= -\frac{V_H t}{I_x B_z} \\ &= -\frac{v_x B_z w t}{n t w v_x e B_z} \\ &= -\frac{1}{ne} \end{aligned} \tag{13.40}$$

depends on carrier density and charge

13.3.2 Quantum

quantum Hall effect

Von Klitzing, Klaus. "The quantized Hall effect." Reviews of Modern Physics 58, no. 3 (1986): 519.

two-dimensional electron gas, high field

quantized cyclotron orbits

fill Landau levels

quantized resistance

$$R_H = \frac{1}{i}\frac{h}{e^2} \tag{13.41}$$

for integer steps i

13.4 SPINTRONICS

spintronics

Joshi, V. K. (2016). Spintronics: A contemporary review of emerging electronics devices. Engineering science and technology, an international journal, 19(3), 1503-1513.

[Wolf *et al*., 2001, Žutić *et al*., 2004, Awschalom & Flatté, 2007]

Wolf, S. A., D. D. Awschalom, R. A. Buhrman, J. M. Daughton, S. Von Molnar, M. L. Roukes, A. Yu Chtchelkanova, and D. M. Treger. "Spintronics: a spin-based electronics vision for the future." science 294, no. 5546 (2001): 1488-1495.

Zutic, Igor, Jaroslav Fabian, and S. Das Sarma. "Spintronics: Fundamentals and applications." Reviews of modern physics 76, no. 2 (2004): 323.

Awschalom, David D., and Michael E. Flatt. "Challenges for semiconductor spintronics." Nature physics 3, no. 3 (2007): 153.

magnetoristance

[Thomson, 1857]

Thomson, William. "XIX. On the electro-dynamic qualities of metals:Effects of magnetization on the electric conductivity of nickel and of iron." Proceedings of the Royal Society of London 8 (1857): 546-550.

GMR, CMR

[Ramirez, 1997]

Ramirez, A. P. "Colossal magnetoresistance." Journal of Physics: Condensed Matter 9, no. 39 (1997): 8171.

spin injection

ferromagnet metal [Johnson & Silsbee, 1985]

semiconductor [Hammar *et al*., 1999]

Johnson, Mark, and Robert H. Silsbee. "Interfacial charge-spin coupling: Injection and detection of spin magnetization in metals." Physical Review Letters 55, no. 17 (1985): 1790.

Hammar, P. R., B. R. Bennett, M. J. Yang, and Mark Johnson. "Observation of spin injection at a ferromagnet-semiconductor interface." Physical Review Letters 83, no. 1 (1999): 203.

spin valve [Dieny *et al*., 1991, Jedema *et al*., 2001]

Dieny, Bernard, Virgil S. Speriosu, Stuart SP Parkin, Bruce A. Gurney, Dennis R. Wilhoit, and Daniele Mauri. "Giant magnetoresistive in soft ferromagnetic multilayers." Physical Review B 43, no. 1 (1991): 1297.

Jedema, F. J., A. T. Filip, and Bart van Wees. "Electrical spin injection and accumulation at room temperature in an all-metal mesoscopic spin valve." J. Supercond 15 (2002): 27-35.

magnetic tunnel junctions

[Zhua & Park, 2006]

Zhu, Jian-Gang Jimmy, and Chando Park. "Magnetic tunnel junctions." Materials today 9, no. 11 (2006): 36-45.

MRAM

[Tehrani *et al*., 1999]

Tehrani, Said, J. M. Slaughter, E. Chen, M. Durlam, J. Shi, and M. DeHerren. "Progress and outlook for MRAM technology." IEEE Transactions on Magnetics 35, no. 5 (1999): 2814-2819.

spin field-effect transistor SFET

[Datta & Das, 1990]

Datta, Supriyo, and Biswajit Das. "Electronic analog of the electrooptic modulator." Applied Physics Letters 56, no. 7 (1990): 665-667.

13.5 SELECTED REFERENCES

[Hummel, 1993] Hummel, Rolf E. (1993). *Electronic Properties of Materials*. 2nd edn. Berlin: Springer-Verlag.

An applied introduction to the magnetic (as well as many other kinds of) properties of materials.

[Mattis, 1988] Mattis, Daniel C. (1988). *The Theory of Magnetism I: Statics and Dynamics*. New York: Springer-Verlag.

The quantum mechanical theory of magnetism.

[O'Handley, 1999] O'Handley, Robert C. (1999). *Modern Magnetic Materials: Principles and Applications*. Hoboken, NJ: Wiley-Interscience.

Magnetic materials and their applications.

[Mee & Daniel, 1996] Mee, C. Denis, & Daniel, Eric D. (eds). (1996). *Magnetic Storage Handbook*. 2nd edn. New York: McGraw-Hill.

[Mallinson, 1993] Mallinson, John C. (1993). *The Foundations of Magnetic Recording*. 2nd edn. Boston: Academic Press.

These two books cover details of practical magnetic storage systems.

13.6 PROBLEMS

(13.1) (*a*) Estimate the diamagnetic susceptibility of a typical solid.
(*b*) Using this, estimate the field strength needed to levitate a frog, assuming a gradient that drops to zero across the frog. Express your answer in teslas.

(13.2) Estimate the size of the direct magnetic interaction energy between two adjacent free electrons in a solid, and compare this to size of their electrostatic interaction energy. Remember that the field of a magnetic dipole $\vec{m}$ is

$$\vec{B} = \frac{\mu_0}{4\pi}\left[\frac{3\hat{x}(\hat{x}\cdot\vec{m}) - \vec{m}}{|\vec{x}|^3}\right] \quad . \tag{13.42}$$

(13.3) Using the equation for the energy in a magnetic field, describe why:
(*a*) A permanent magnet is attracted to an unmagnetized ferromagnet.
(*b*) The opposite poles of permanent magnets attract each other.

(13.4) Estimate the saturation magnetization for iron at 0 K.

(13.5) (*a*) Show that the area enclosed in a hysteresis loop in the (B,H) plane is equal to the energy dissipated in going around the loop.
(*b*) Estimate the power dissipated if 1 kg of iron is cycled through a hysteresis loop at 60 Hz; the coercivity of iron is 4×10^3 A/m.

(13.6) Approximately what current would be required in a straght wire to be able to erase a γ-Fe_2O_3 recording at a distance of 1 cm?